

INTEGRATED NEURAL PROCESSES FOR DEFINING POTENTIAL ACTIONS AND DECIDING BETWEEN THEM: A COMPUTATIONAL MODEL

Paul Cisek

Department of physiology
University of Montréal
C.P. 6128 Succursale Centre-ville
Montréal, Québec H3C 3J7 Canada
Phone: 514-343-6111 x4355
FAX: 514-343-2111
e-mail: paul.cisek@umontreal.ca

Supplemental Material

Modeling approach

In any modeling effort, one is faced with a tradeoff between tractability and physiological realism. The model presented below is aimed at implementing the hypotheses described in the main text at a level of detail just sufficient to capture the neurophysiological and behavioral phenomena of interest. These phenomena include response patterns over populations of cells in specific regions of the cerebral cortex, but do not include the precise spiking behavior of individual cell types in individual cortical layers. Thus, neural activity is represented simply as average firing rates (as opposed to membrane potentials or spikes), which rise and fall as non-linear functions of excitation, inhibition, and noise. Each cortical region is implemented as a homogeneous population of neurons which differ only in terms of directional tuning and in terms of random variations of weight parameters. However, despite this abstract representation of individual neurons, the model is able to generate patterns of activity which capture many of the features of real cortical activation and to make predictions about how cells in specific regions will respond under novel experimental conditions.

The model focuses primarily on the dynamics of neural activity in dorsal premotor and posterior parietal cortex, and simplifies many details of the dynamics of activity outside those emphasized regions. For example, no visual processing is included in the model, and we simply assume that potential target directions are presented to PPC as input. We also do not address the question of the coordinate system used by each region and for simplicity encode everything as a spatial direction. Likewise, the dynamics of prefrontal processing is significantly simplified. We do not simulate or address how the prefrontal cortex learns to detect relevant stimulus information and to combine that with a cognitive knowledge of the task at hand – we simply assume that PFC cells receive the correct information as input. We implement the gradual accumulation of sensory evidence in PFC cells in an “ad-hoc” manner by simply by giving them the dynamics of leaky-integrators with a slow time constant. Future modeling work may expand these abstractions to produce a more realistic picture of real prefrontal processing. For example, gradual integration may be accomplished by replacing the slow PFC time constant with a network of neurons with positive feedback made robust to noise using bistable dendrites (Goldman et al., 2003), and maintenance of a stable working memory in PFC may be implemented via recurrent synaptic interactions and more detailed cellular properties (Compte et al., 2000). However, a detailed model of prefrontal processing is not the object of the present study. The goal of the present modeling work is more humble – to implement the hypotheses described in the main text through a set of mathematical equations which allow us to test specific predictions in more detail than is possible without a formal model.

Mathematical methods

The model was implemented as a dynamical system describing mean-rate leaky-integrator neurons arranged in seven layers of 90 units each. Following Grossberg (1968;1973), each neuron was governed by the following non-linear differential equation:

$$\frac{dX_i^L}{dt} = -\alpha X_i^L + (\beta - X_i^L) \gamma \cdot E_i^L - X_i^L \cdot I_i^L + \Theta(0, \eta) \quad (1)$$

where X_i^L is the activity of the i th neuron of a given layer L , $\frac{dX_i^L}{dt}$ is the change in that activity over time, E_i^L is the excitatory input to the neuron, I_i^L is the inhibitory input, α is the decay rate, β is the neuron's maximum activity, and γ is the excitatory gain. Noise Θ was modeled as Gaussian noise with mean 0 and variance η . The output Y_i^L of each neuron was thresholded such that

$$Y_i^L = [X_i^L - \Gamma]^+$$

where $[w]^+$ is defined as $\max(w, 0)$.

Every neuron in the model obeyed the dynamics of equation (1). Most neurons used the same parameters: $\alpha = 3$, $\beta = 2$, $\gamma = 6$, $\eta = 0.1$, and $\Gamma = 0.1$. The exceptions were as follows: PPC neurons used $\Gamma^{PPC} = 0.5$, and PFC neurons used $\alpha^{PFC} = 0.01$, $\beta^{PFC} = 4$, $\gamma^{PFC} = 0.1$, $\eta = 0.15$, and $\Gamma^{PFC} = 0.2$. Importantly, these values gave PFC neurons slower growth and decay dynamics in relation to PPC and PMd neurons (see above for justification of this simplified approach).

The behavior of individual model layers was distinguished by the pattern of connections with other layers in the network, expressed through the excitation and inhibition terms.

For PPC, these terms were defined as follows:

$$\begin{aligned} E_i^{PPC} &= V_i^N + \sum_j w_{ji}^{PMd \leftrightarrow PPC} \cdot Y_j^{PMd1} + 0.5 \cdot \sum_j KE_{ji} \cdot g(Y_j^{PPC}) \\ I_i^{PPC} &= 0.5 \cdot \sum_j KI_{ji} \cdot g(Y_j^{PPC}) \\ g(w) &= w^{0.6} \end{aligned} \quad (2)$$

where Y_j^{PMd1} is the output of the j th cell in the top PMd layer, $w_{ji}^{PMd \leftrightarrow PPC}$ is the synaptic weight between the j th unit in PMd and the i th unit in PPC, KE and KI are the excitatory and inhibitory kernels representing the lateral connections between cells within the layer (see below), and $g(w)$ is a transfer function describing how activity of one PPC cell affects the activity of another (See Figure S1). The term V_i^N is the visual input to PPC, which is equal to the magnitude of visual input at the i th unit's preferred location. The superscript N denotes that visual input to PPC is not category selective.

Equations (2) state that PPC cells are excited by visual input, feedback from PMd, and lateral excitation within PPC, and inhibited by lateral inhibition within PPC. The connection weights $w_{ji}^{PMd \leftrightarrow PPC}$ were hard-wired such that $w_{ji}^{PMd \leftrightarrow PPC} = 0.4$ for $j=i$, and then fell off linearly to reach zero when $|j-i| > 2$. The weights were then randomized with 1% Gaussian noise.

The lateral interaction kernel was defined as a Difference-of-Gaussians function

$$\begin{aligned} K_d &= \kappa \cdot \left(\frac{e^{-d^2/2}}{\sqrt{2\pi}} - 0.4 \cdot \frac{e^{-d^2/8}}{\sqrt{2\pi}} \right) - \rho \\ KE_{ji} &= [K_{\sigma(j-i)}]^+ \\ KI_{ji} &= [-K_{\sigma(j-i)}]^+ \end{aligned} \quad (3)$$

Additional randomness was introduced into the model by modifying each layer's kernel of interactions with 20% Gaussian noise. The kernel parameters were set at $\kappa = 1.75$, $\rho = 0.25$, $\sigma = 0.1$. The lateral interactions implemented through this kernel "wrapped-around" in each layer from one edge to the other, in order to capture the inherent circular nature of directional tuning.

The PFC was implemented as two separate groups of 90 cells, each of which was selective for a particular category C . Although for display purposes these cells were sorted by their preferred location, there were no lateral interactions between them, and thus no topology. Therefore, they could be arranged in any arbitrary and even random organization. PFC excitation and inhibition were defined as:

$$\begin{aligned} E_i^{PFC} &= 0.1 \cdot V_i^C \\ I_i^{PFC} &= \sum_j w_{ji}^{PFC} \cdot Y_j^{PFC} \end{aligned} \quad (4)$$

where V_i^C is the magnitude of visual input corresponding to the neuron's preferred category C near location i within a distance of 10 units. Hence PFC neurons have very low spatial resolution. The inhibitory term states that PFC neurons with different category preferences inhibit each other with $w_{ji}^{PFC} = 0.1$ when $j=i$. As described above, these equations implement a signal which resembles the behavior of PFC (Kim and Shadlen, 1999) but should not be construed as hypotheses on how the PFC computes that signal.

The dorsal premotor cortex was simulated as a set of three layers of 90 cells each, which had the following excitation and inhibition functions:

$$\begin{aligned} E_i^{PMd1} &= \sum_j w_{ji}^{PMd \leftrightarrow PPC} \cdot Y_j^{PPC} \cdot PFC_{ji} + \sum_j w_{ji} \cdot Y_j^{PMd2} + \sum_j KE_{ji} \cdot f(Y_j^{PMd1}) \\ I_i^{PMd1} &= \sum_j KI_{ji} \cdot f(Y_j^{PMd1}) \end{aligned} \quad (5)$$

$$\begin{aligned} E_i^{PMd2} &= \sum_j w_{ji} \cdot Y_j^{PMd1} + \sum_j w_{ji} \cdot Y_j^{PMd3} + \sum_j KE_{ji} \cdot f(Y_j^{PMd2}) \\ I_i^{PMd2} &= \sum_j KI_{ji} \cdot f(Y_j^{PMd2}) \end{aligned} \quad (6)$$

$$\begin{aligned} E_i^{PMd3} &= \sum_j w_{ji} \cdot Y_j^{PMd2} + \sum_j w_{ji} \cdot Y_j^{M1} + \sum_j KE_{ji} \cdot f(Y_j^{PMd3}) \\ I_i^{PMd3} &= \sum_j KI_{ji} \cdot f(Y_j^{PMd3}) \end{aligned} \quad (7)$$

where all the weights w_{ji} between layers were hard-wired such that $w_{ji} = 0.2$ for $j=i$, and then fell off linearly to zero when $|j-i| > 2$ (again with 1% Gaussian noise), and the kernel of interactions was defined as in (3).

Two observations can be made regarding equations (5-7). First, each PMd layer receives excitatory input from the layer upstream as well as from the layer downstream. All of these are connected through similar weight matrices with one important exception. The excitation that the uppermost layer of PMd receives from PPC is multiplicatively modulated by input from PFC. This modulation was defined as:

$$PFC_{ji} = w_{ji}^{PFC \rightarrow PMd} \cdot \left[\left(Y_j^{PFC^R} \right)^2 + \left(Y_j^{PFC^B} \right)^2 \right] + \omega \quad (8)$$

The weights were such that $w_{ji}^{PFC \rightarrow PMd} = 0.15$ when $j=i$ and fell off linearly to reach zero when $|j-i| > 10$. This means that the resolution of projections from PFC to PMd1 was very low, as low as the spatial resolution of visual input to PFC (4).

The reason for the multiplicative interaction is to prevent PFC cells from exciting PMd1 on their own in the absence of PPC activity. However, PPC can on its own excite PMd1, even without PFC input, because the parameter ω was set at 0.5. The multiplicative gating of the input to PMd1 expresses the idea that PFC can bias the competition in PMd. While it is consistent with a number of reports of multiplicative

interactions between variables encoded in the firing of cortical cells (Andersen, 1995; Kalaska et al., 1989), it is not proposed as a specific hypothesis of a particular mechanism at the level of individual synapses.

The second observation regarding equations (5-7) is that the lateral interactions between cells within each PMd layer are determined not only by the kernel K but also by an interaction function $f()$, defined as:

$$f(x) = \frac{1}{0.3 + e^{-4(x-1.3)}} + 0.3 \quad (9)$$

This function is the sigmoidal transfer function shown in Figure 1c. It implements the quenching dynamics described in the text, because as a cell's activity gets large, it begins to exert more and more excitation on its neighbors and more and more inhibition on the rest of the layer. The precise functional form of $f()$ is not critical as long as it contains a faster-than-linear portion for large values of x . See Grossberg (1973) for further discussion and proofs concerning the dynamics of a general class of non-linear recurrent networks of which this is a special case.

The excitation and inhibition of primary motor cortex was defined as:

$$\begin{aligned} E_i^{M1} &= \sum_j w_{ji} \cdot Y_j^{PMd3} \cdot GO + 2.25 \cdot \sum_j KE_{ji} \cdot (Y_j^{M1})^2 \\ I_i^{M1} &= 2.25 \cdot \sum_j KI_{ji} \cdot (Y_j^{M1})^2 \end{aligned} \quad (10)$$

In other words, M1 cells are excited by output from the bottom layer of PMd whenever the GO signal is above zero. The multiplicative gating of the excitatory input to M1, like the multiplicative gating of the PPC input to PMd, is simply mathematical shorthand for the idea that activation of M1 and the initiation of movement can be decoupled from activity in upstream brain regions (Bullock and Grossberg, 1988; Bullock et al., 1998).

Individual cells in M1 also engage in strong lateral interactions which are governed by a faster-than-linear function (2nd power). These strong lateral interactions cause M1 to exhibit strong winner-take-all dynamics, which force a choice any time distinct peaks of activity appear.

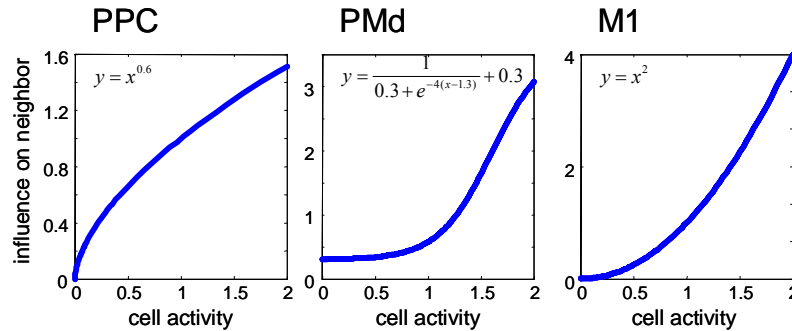


Figure S1. The lateral influence of a cell on neighboring cells in the same population as a function of current activity.

Parametric sensitivity

A numerical analysis of parameter sensitivity was conducted using an iterative random walk procedure through the space of ten of the model's parameters: α , β , γ , κ , ρ , σ , ω , W , $W^{PPC \leftrightarrow PMd}$, $W^{PFC \rightarrow PMd}$. In each iteration, one of the parameters was randomly varied to either increase or decrease, and a simulation of the 2-target task was performed. If the model performed well (according to the criterion defined below), then a new iteration was performed. If the model did not perform well, then the changed parameter was returned to its previous value and a different parameter change was attempted. After 20 consecutive failures the procedure the model was considered to have reached a "dead-end" in parameter space and was re-initialized from a new starting position. This procedure was run for 10000 simulations of the 2-target task.

Performance in each simulation was evaluated using the following function:

$$P = \frac{[2Y_{30}^{PMd1}(t_{CC}) - Y_{45}^{PMd1}(t_{CC}) - Y_{75}^{PMd1}(t_{CC})]^+}{2Y_{30}^{PMd1}(t_{CC}) + Y_{45}^{PMd1}(t_{CC}) + Y_{75}^{PMd1}(t_{CC})} \cdot \frac{[2Y_{60}^{PMd1}(t_{CC}) - Y_{45}^{PMd1}(t_{CC}) - Y_{75}^{PMd1}(t_{CC})]^+}{2Y_{60}^{PMd1}(t_{CC}) + Y_{45}^{PMd1}(t_{CC}) + Y_{75}^{PMd1}(t_{CC})} \cdot \frac{[Y_{30}^{PMd3}(t_{GO}) - Y_{60}^{PMd3}(t_{GO})]^+}{Y_{30}^{PMd3}(t_{GO}) + Y_{60}^{PMd3}(t_{GO})} \quad (11)$$

The first two terms of this function evaluate the strength of bimodal activity in PMd1 at the time the color cue is presented t_{CC} , and the third term evaluates how well the model chose the correct target by the time of the GO signal t_{GO} . Each term in the product is normalized, yielding a function P which measures performance on a positive scale. The criterion for successful performance was $P > 0.1$.

This procedure found that the model has a large region within the tested parameter space in which it

Parameter	Symbol	Start	Minimum	Maximum
Decay rate	α	3.00	0.12	5.90
Maximum activity	β	2.00	0.50	3.82
Excitatory gain	γ	6.00	0.25	10.69
Kernel gain	κ	1.75	0.53	4.91
Kernel baseline	ρ	0.25	0.018	0.52
Kernel width scale	σ	0.10	0.057	0.66
PFC→PMd baseline	ω	0.50	0.011	0.95
Weights (mean)	w	0.20	0.06	0.61
PPC↔PMd weights	$w^{PPC \leftrightarrow PMd}$	0.40	0.12	0.86
PFC→PMd weights	$w^{PFC \rightarrow PMd}$	0.15	0.051	0.54

Table S1: Range of model parameter values for which successful simulations of the 2-target task were found during a random-walk of 10,000 steps.

performs adequately. Of the 10,000 simulations which were run, 5719 met the criterion for success and a dead-end was reached only 11 times during these simulations. As shown in Table S1, the range of values of each parameter for which successful performance was obtained was large and for most parameters spanned one or two orders of magnitude. In conclusion, the analysis shows that the model is robust and not dependent on precise fine-tuning of each parameter.

Reference List

1. Andersen RA (1995) Encoding of intention and spatial location in the posterior parietal cortex. *Cereb Cortex* 5: 457-469.
2. Bullock D, Cisek P, Grossberg S (1998) Cortical networks for control of voluntary arm movements under variable force conditions. *Cereb Cortex* 8: 48-62.
3. Bullock D, Grossberg S (1988) Neural dynamics of planned arm movements: Emergent invariants and speed-accuracy properties during trajectory formation. *Psychological Review* 95: 49-90.
4. Compte A, Brunel N, Goldman-Rakic PS, Wang XJ (2000) Synaptic mechanisms and network dynamics underlying spatial working memory in a cortical network model. *Cereb Cortex* 10: 910-923.
5. Goldman MS, Levine JH, Major G, Tank DW, Seung HS (2003) Robust persistent neural activity in a model integrator with multiple hysteretic dendrites per neuron. *Cereb Cortex* 13: 1185-1195.
6. Grossberg S (1968) Some physiological and biochemical consequences of psychological postulates. *Proceedings of the National Academy of Sciences* 60: 758-765.
7. Grossberg S (1973) Contour enhancement, short term memory, and constancies in reverberating neural networks. *Studies in Applied Mathematics* 52: 213-257.
8. Kalaska JF, Cohen DAD, Hyde ML, Prud'homme MJ (1989) A comparison of movement direction-related versus load direction-related activity in primate motor cortex, using a two-dimensional reaching task. *J Neurosci* 9: 2080-2102.
9. Kim J-N, Shadlen MN (1999) Neural correlates of a decision in the dorsolateral prefrontal cortex of the macaque. *Nat Neurosci* 2: 176-185.